LPA receptor 4 deficiency attenuates experimental atherosclerosis[S]

Liping Yang,* Maria Kraemer,* Xianjun Frank Fang,[†] Peggi M. Angel,[§] Richard R. Drake,[§] Andrew J. Morris,*, and Susan S. Smyth[1,*,**]**

Division of Cardiovascular Medicine,* Gill Heart and Vascular Institute, University of Kentucky, Lexington, KY 40536; Department of Biochemistry and Molecular Biology,[†] VCU Massey Cancer Center, Virginia Commonwealth University, Richmond, VA 23298-0614; Department of Cell and Molecular Pharmacology,[§] MUSC Proteomics Center, Medical University of South Carolina, Charleston, SC 29425; and Veterans Affairs Medical Center,** Lexington, KY 40511

Abstract **The widely expressed lysophosphatidic acid (LPA) selective receptor 4 (LPAR4) contributes to vascular development in mice and zebrafish. LPAR4 regulates endothelial permeability, lymphocyte migration, and hematopoiesis, which could contribute to atherosclerosis. We investigated the role of LPAR4 in experimental atherosclerosis elicited by adeno-associated virus expressing PCSK9 to lower LDL receptor levels. After 20 weeks on a Western diet, cholesterol levels and lipoprotein distribution were similar in WT male and *Lpar4*$^{Y/-}$ mice ($P = 0.94$). The atherosclerotic lesion area in the proximal aorta and arch was ~25% smaller in *Lpar4*$^{Y/-}$ mice ($P = 0.009$), and less atherosclerosis was detected in *Lpar4*$^{Y/-}$ mice at any given plasma cholesterol. Neutral lipid accumulation in aortic root sections occupied ~40% less area in *Lpar4*$^{Y/-}$ mice ($P = 0.001$), and CD68 expression was ~25% lower ($P = 0.045$). No difference in α-smooth muscle actin staining was observed. Bone marrow-derived macrophages isolated from *Lpar4*$^{Y/-}$ mice displayed significantly increased upregulation of the M2 marker *Arg1* in response to LPA compared with WT cells. In aortic root sections from *Lpar4*$^{Y/-}$ mice, heightened M2 "repair" macrophage marker expression was detected by CD206 staining ($P = 0.03$).** These results suggest that LPAR4 may regulate the recruitment of specific sets of macrophages or their phenotypic switching in a manner that could influence the development of atherosclerosis.—Yang, L., M. Kraemer, X. F. Fang, P. M. Angel, R. R. Drake, A. J. Morris, and S. S. Smyth. **Lysophosphatidic acid receptor 4 deficiency attenuates experimental atherosclerosis.** ***J. Lipid Res.*** **2019.** 60: **972–980.**

Supplementary key words lysophospholipids • lipid phosphate phosphatase • lysophosphatidic acid

Lysophosphatidic acid (LPA) and several other related molecules constitute a family of bioactive lipid phosphoric acids that function as receptor-active mediators with roles in cell growth, differentiation, apoptosis, and development (1–5). Vascular smooth muscle (6, 7), vascular endothelial cells (8), and platelets (9, 10) are notably responsive to LPA (11, 12). LPA, a potent trigger for Rho activation, promotes endothelial cell migration, disrupts endothelial barrier function, and induces the phenotypic modulation of vascular smooth muscle cells (SMCs). In addition to its effects on endothelial cells (13, 14) and SMCs (6, 7), LPA is a weak activator of platelets (9, 10) and a potent stimulus for fibronectin matrix assembly (15). LPA promotes inflammatory responses in endothelial cells and leukocytes (16) and triggers neutral lipid accumulation in monocytes (17). The effects of LPA are largely mediated by members of a family of G protein-coupled receptors with six putative members [LPA receptors (LPARs) 1–6] (1–4). Ongoing efforts seek to define the role of specific LPARs in blood and vascular cell functions in development and disease.

LPA is present in the lipid-rich core of human atheroma, and levels increase in lesions in mice during the progression of atherosclerosis (18, 19). Advanced lesions in Ldlr$^{-/-}$ mice, generated by a combination of diet and collar placement around the carotid artery, contain ~20-fold higher levels of LPA than uninjured vessels, especially highly unsaturated long-chain acyl-LPA species (20), and may be influenced by cholesterol feeding (21). Multiple LPA species can be detected by mass spectrometry-based analysis of lipid-extraction imaging of human and murine atheroma. Sampling of blood from coronary arteries at the

This study was supported by National Institutes of Health Grant R01 HL120507 and US Department of Veterans Affairs Grant BX002769.

Manuscript received 9 November 2018 and in revised form 14 February 2019.

Published, JLR Papers in Press, February 22, 2019
DOI https://doi.org/10.1194/jlr.M091066

Abbreviations: AAV, adeno-associated virus; BMDM, bone marrow-derived macrophage; KLF, Krüppel-like factor; LPA, lysophosphatidic acid; LPAR, lysophosphatidic acid receptor; ox-LDL, oxidized LDL; PLA, proximity ligation assay; SMC, smooth muscle cell; SRA, scavenger receptor class A.

[1]To whom correspondence should be addressed.
e-mail: susansmyth@uky.edu

[S] The online version of this article (available at http://www.jlr.org) contains a supplement.

time of acute myocardial infarction reveals higher local levels of LPA (22). Hyperlipidemia may also increase steady-state levels of LPA in plasma and/or enhance the capacity for LPA synthesis. Studies in rabbits suggest that systemic LPA levels may be influenced by cholesterol feeding, which elevates plasma levels of the LPA precursor lysophosphatidylcholine and heightens the generation of LPA in serum (21). Recent work supports a link between levels of LPA in the small intestine and experimental atherosclerosis, and feeding mice a diet supplemented with unsaturated LPA mimics the inflammatory effects of the Western diet (23).

LPA may promote experimental atherosclerosis in a receptor-dependent manner. Treatment of $Apoe^{-/-}$ mice with LPA promotes monocyte adhesion to the endothelium, stimulates perivascular macrophage accumulation, and heightens atherosclerotic plaque burden in an LPAR1- and LPAR3-dependent manner (8). Similarly, pharmacological antagonism of LPAR1/LPAR3 alters inflammatory cell profiles in $Ldlr^{-/-}$ mice and retards the progression of atherosclerosis (24). Due in part to the lack of selective pharmacologic tools for targeting specific receptors, whether other LPARs also contribute to atherosclerosis is not known. Reports in both mice and zebrafish have clearly established a role for a particular LPA receptor subtype, LPAR4, in vascular development (25, 26) and vascular network formation by promoting cell-cell contact (27, 28). LPAR4 may also regulate lymphocyte transmigration (29) and influence hematopoiesis (30). These effects could contribute to atherosclerosis development. Therefore, we sought to understand the role of LPAR4 in the development of experimental atherosclerosis.

METHODS

Mice

All procedures conformed to the recommendations of the National Institutes of Health *Guide for the Care and Use of Laboratory Animals* and were approved by the Institutional Animal Care and Use Committee. Mice lacking Lpar4 have previously been described (31) and were backcrossed to the C57BL/6J mice (The Jackson Laboratory, Bar Harbor, ME, Stock # 000664), as the phenotype in the mice is dependent on the genetic background, with approximately one-third of the mice dying before birth or weaning (25). All study mice were maintained in individually vented cages (maximum of five mice per cage) on a 14-h light and 10-h dark cycle and euthanized 2–4 h after the end of the dark cycle. Mice were fed a normal rodent laboratory diet (Diet # 2918, Envigo Teklad, Huntingdon, UK) and provided with drinking water from a reverse-osmosis system ad libitum. Immediately after adeno-associated virus (AAV) injections, mice were fed a Western diet containing saturated fat [21% (w/w) milk fat; Diet # TD.88137, Harlan Teklad] for 20 weeks unless otherwise stated.

Hyperlipidemia

AAV vectors (serotype 8) were produced by the Viral Vector Core at the University of Pennsylvania. These AAV vectors contained inserts expressing the mouse PCSK9D377Y mutation (equivalent to the human PCSK9D374Y gain-of-function mutation). AAV vectors were diluted in sterile PBS (200 µl per mouse) and injected intraperitoneally (2×10^{11} genomic copies) as previously reported (30). Total plasma cholesterol was measured using the Cholesterol E Assay (Wako Diagnostics, Mountain View, CA; Cat#439-175001) according to the manufacturer's protocol. Plasma lipoprotein cholesterol distributions were determined by fast-performance LC. Plasma (50 µl) was separated using a Superose 6 size-exclusion fast-performance LC column. Cholesterol concentrations were determined by an enzymatic colorimetric assay in fractions collected from the column eluate. Mice with cholesterol levels <500 mg/dl were excluded from atherosclerosis analysis.

Atherosclerosis analysis

For en face atherosclerosis analysis, aortas were cleaned of the adventitia, dissected from the aortic root to the iliac bifurcation, and stored in 10% formalin for 24–48 h. Aortas were then transferred to a 0.9% saline solution and stored at 4°C for at least 1 day. Aortas were cut open longitudinally, exposing the intimal surface, and secured with pins to be photographed. Atherosclerosis was quantified on the intimal surface of the ascending aorta, aortic arch, and from the aortic orifice of the left subclavian artery to 3 mm below by the en face technique as previously described (32).

For microscopic analysis of atherosclerosis at the aortic root, serial sections were taken at 10 µm intervals. Slides were fixed by immersion in chilled acetone at −20°C for 10 min. CD68 was detected with primary antibody (Abcam, Cambridge, MA; Cat# ab53444; 1:100) and secondary biotin-conjugated antibody, amplified by the VECTASTAIN ABC detector kit (Vector Laboratories, Burlingame, CA), and visualized by enzymatic precipitation of a chromogen substrate (VECTOR NovaRED substrate kit; Vector Laboratories). For α-smooth muscle actin, antibody staining (Sigma-Aldrich, St. Louis, MO; A-5691; 1:100) was detected with the Vector Red substrate kit (Vector Laboratories, sk-5100). The areas were quantified using MetaMorph software (Molecular Devices, San Jose, CA). For the detection of neutral lipid content in the atherosclerosis plaque, aortic root sections were stained with Oil Red O and counterstained with hematoxylin. Atherosclerotic lesions were measured by manually tracing lesion areas on each section as previously described (32). Measurements were made from six serial sections taken at 80 µm intervals, and the average was reported for each mouse. Antibody controls are included in supplemental Fig. 2. In situ hybridization and proximity ligation assays (PLAs) were performed as previously described (33). Imaging was performed using a Nikon (Melville, NY) A1R confocal microscope with a spectral detector, and analysis was performed using Nikon's NIS software.

Isolation and culture of cells

Bone marrow-derived macrophages (BMDMs) were isolated from the mice by flushing the femur and tibia with DMEM. The bone marrow cells were resuspended in DMEM supplemented with 10% FBS, 1% Pen/Strep, and 10% L929-conditioned media containing macrophage colony-stimulating factor and plated at a density of 1×10^6/well in a six-well plate. Cells were incubated for 7 days at 37°C and 5% CO_2, and the medium was changed every 2–3 days. BMDMs were serum-starved for 12 h in 0.1% FBS and 1% Pen/Strep and then stimulated with LPA (5 µM; Avanti Polar Lipids, Alabaster, AL) or oxidized LDL (ox-LDL) (50 µg/ml; Kalen Biomedical, Germantown, MD) or vehicle for 3 h.

Tissues, including aorta, were stored in RNAlater (QIAGEN, Frederick, MD) and homogenized by mortar and pestle, and total RNA was extracted using TRIzol (ThermoFisher Scientific, Waltham, MA) following the manufacturer's instructions. cDNA was prepared with MultiScribe reverse-transcriptase enzyme (High

Capacity cDNA Reverse Transcription Kit; ThermoFisher Scientific) according to the manufacturer's directions. All probes used in the study spanned an exon junction and thus would not detect genomic DNA. An RNA sample without reverse transcription was used as a negative control. Samples were assayed using QuantStudio 7 Flex (ThermoFisher Scientific). Threshold cycles were determined by an in-program algorithm assigning a fluorescence baseline based on readings prior to exponential amplification. Fold change in expression was calculated with the 2-δδCT method using 18s RNA as an endogenous control. The TaqMan® gene expression (ThermoFisher Scientific) primers used are listed in supplemental Table 1.

Statistics

All results are expressed as means ± SDs. Statistical significance within strains was determined using Student's *t*-test or two-way ANOVA with multiple pairwise comparisons as appropriate. In *t*-tests, if a sample failed the normality test, a rank *t*-test was used. In some cases of two-way ANOVA, data were log-transformed to be normally distributed. Statistical analysis was performed using SigmaPlot version 13 software. $P < 0.05$ was considered significant.

RESULTS

LPA levels increase during experimental atherosclerosis in mice (supplemental Fig. 1). To investigate a role for LPAR4 signaling in the development of experimental atherosclerosis, hyperlipidemia was elicited by infecting mice with AAV expressing a gain-of-function allele of the PCSK9 D377Y mutation (PCSK9D377Y.AAV) to lower LDL receptor levels and concurrently feeding mice a Western diet to increase plasma cholesterol. LPAR4 deficiency had no effect on the development of hypercholesterolemia (**Fig. 1A**). Cholesterol levels in WT male mice (n = 20) and *Lpar4*$^{Y/-}$ mice (n = 10) were 839 ± 176 and 844 ± 158 mg/dl, respectively (P = 0.94). No difference in the cholesterol lipoprotein distribution by size-exclusion chromatography was observed between the genotypes (Fig. 1B). Complete blood counts were also similar in the two genotypes (supplemental Table 2).

The atherosclerotic lesion area was measured on the intimal surfaces of the proximal aorta and arch by en face analyses (Fig. 1C). The lesion area to total aortic area was significantly greater in male WT mice (0.318 ± 0.06) than in *Lpar4*$^{Y/-}$ mice (0.235 ± 0.08; P = 0.009; Fig. 1D). To exclude the possibility that the variability in plasma cholesterol levels after PCSK9D377Y.AAV treatment affected the development of atherosclerosis independent of genotype, we examined the relationship between total cholesterol and the extent of atherosclerosis measured by en face analysis (Fig. 1E). In both WT and *Lpar*$^{4Y/-}$ mice, a linear correlation between plasma cholesterol and the extent of atherosclerosis was observed. However, even with normalization to plasma cholesterol levels, relatively less atherosclerosis was detected in *Lpar4*$^{Y/-}$ mice compared with WT controls.

To gain insight into the potential mechanisms underlying these effects on atherosclerosis, we examined the cellular composition of lesions. Consistent with the en face analysis, neutral lipid accumulation, as detected by Oil Red O staining, was significantly lower in serial sections taken at the aortic root of *Lpar4*$^{Y/-}$ mice (**Fig. 2A**). The area of Oil Red O staining was 0.547 ± 0.08 mm^2 in the WT mice (n = 10) and 0.348 ± 0.122 mm^2 in the knockout mice (n = 11) (P = 0.001). Macrophage accumulation and/or the transdifferentiation of cells to a macrophage-like phenotype, as detected by CD68 expression, was also lower in the receptor-deficient mice (Fig. 2B), with an area of 2,669 ± 699 units in WT mice (n = 10) and 2,024 ± 380 units in *Lpar4*$^{Y/-}$ mice (n = 7) (P = 0.045). No differences in SMC area, as detected by α-smooth muscle actin staining, was observed between WT (470 ± 208 units; n = 10) and knockout mice (591 ± 229 units; n = 11) (P = 0.27) (Fig. 2C).

LPAR4 is carried on the X chromosome in mice. We therefore investigated sex differences in the role of the receptor in the development of atherosclerosis. No difference in cholesterol levels after PCSK9D377Y.AAV injection was observed between the genotypes in female mice, although total cholesterol levels in female mice were lower than those achieved in male mice. Median cholesterol levels were 438 mg/dl in WT female mice (n = 27) and 477 mg/dl in *Lpar4*$^{-/-}$ mice (n = 29) (supplemental Fig. 3A). The lesion area to total aortic area in female WT mice (median: 0.05; 25% to 75% CI: 0.05, 0.288) was not significantly different than in female *Lpar4*$^{-/-}$ mice (median: 0.09; 25% to 75% CI: 0.05, 0.317; P = 0.9) (supplemental Fig. 3B). Supplemental Fig. 3C shows the relationship between plasma cholesterol and en face atherosclerosis development in female mice. While these observations may point to a sex difference in the role of LPA signaling, it is important to note that PCSK9D377Y.AAV was less effective at elevating cholesterol levels in female mice. The resulting lower lesion development likely limited our ability to detect a difference between genotypes.

To understand the role of LPAR4 in specific cellular signaling systems of relevance to atherosclerosis, we explored lipid-mediated responses in cells isolated from mice lacking LPAR4. Environmental lipid-induced transformation elicited by treating cells with ox-LDL converts macrophages into lipid-laden foam cells and transdifferentiates SMCs to assume a macrophage-like phenotype. LPA signaling has been implicated in responses that affect foam cell formation (17, 34–37) and SMC phenotypic modulation (38–40). The class B scavenger receptor CD36 and the scavenger receptor class A (SRA) are the major receptors responsible for the binding and uptake of ox-LDL. LPA signaling has been reported to increase SRA (35) and affects CD36 expression in certain circumstances (33). Thus, we examined the role of LPAR4 in these effects and responses to LPA in BMDMs and primary cultures of aortic SMCs from the mice.

After exposure to LPA (**Fig. 3A**), BMDMs express higher levels of *F3* (tissue factor) and *Ctgf* (Fig. 3A), as has been reported in other model systems (41–43). After exposure to ox-LDL, BMDM expression of *Cd36* increases, and the expression of *Il-10* declines. Neither LPA nor ox-LDL significantly altered *Sra1* expression under the experimental conditions examined. Compared with WT cells, LPAR4-deficient cells expressed significantly higher levels of *Arg1*

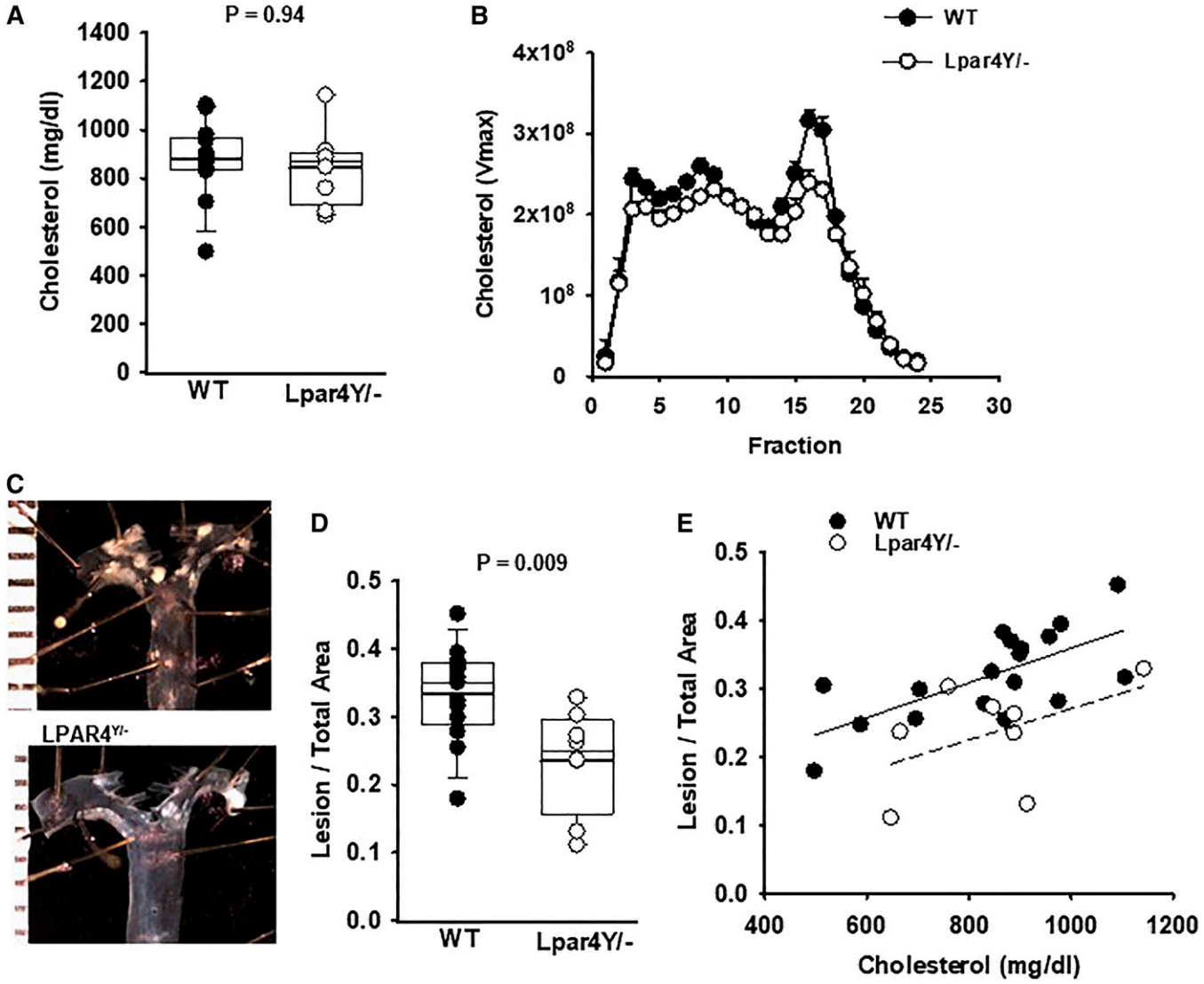

Fig. 1. LPAR4 deficiency in male mice reduces atherosclerosis but has no effect on plasma cholesterol profiles. A: Total cholesterol in plasma from individual WT (dark circles) or *Lpar4*$^{Y/-}$ (open circles) mice infected with PCSK9D377Y.AAV and fed a Western diet for 20 weeks ($P = 0.94$). B: Plasma lipoprotein particles were resolved by size-exclusion chromatography and total cholesterol in the indicated fractions ($n = 3$ mice/genotype determined). C: Images of representative aortas from WT and *Lpar4*$^{Y/-}$ mice. D: En face analysis of atherosclerotic lesions from the ascending aorta to 3 mm below the subclavian artery. The atherosclerotic lesion area/total aortic area for individual WT (dark circles) or *Lpar4*$^{Y/-}$ (open circles) mice is presented ($P = 0.009$). E: Atherosclerosis lesion area plotted as a function of plasma cholesterol in WT (dark circles) or *Lpar4*$^{Y/-}$ (open circles) mice.

mRNA in response to LPA (Fig. 3A; $P < 0.05$). We explored potential mechanisms by examining the expression of Krüppel-like factors (KLFs) 4 and 6, which are transcription factors that regulate the phenotypic modulation of cells and, in the case of KLF4, are reported to be influenced by LPA signaling in other cells. Interestingly, LPA exposure increased KLF4 expression in LPAR4-deficient cells but not WT cells (Fig. 3B), whereas KLF6 was increased in both cell genotypes in response to ox-LDL. Together, these results suggest that LPAR4 may normally regulate phenotypic modulation. ARG1 is a marker of M2 "repair" macrophages, which have been associated with lesion regression (44). To determine whether LPAR4 likewise increased M2 subsets of macrophages within atherosclerotic lesions, staining for the M2 marker CD206 was measured in sections from mice (Fig. 3C). Compared with CD206 in WT ($n = 10$) aortic root sections, the CD206$^+$ area was significantly higher in *Lpar4*$^{Y/-}$ tissue (707 ± 142 vs. 825 ± 102 μm^2; $P = 0.03$). In both genotypes, CD206$^+$ cells were abundant in the adventitial area external to the medial layer; however, LPAR4-deficient mice displayed more CD206$^+$ cells within the atherosclerotic lesions (Fig. 3D, E).

We also investigated the role of LPAR4 in SMC responses. Aortic SMCs isolated from *Lpar4*-deficient mice have virtually no LPAR4 gene expression ($P < 0.001$ vs. WT) (**Fig. 4A**). After exposure to ox-LDL, SMCs upregulate gene expression for the inflammatory markers *Il-6* and *Cd68* ($P = 0.049$ vs. vehicle control), with no difference between WT and null genotypes. Interestingly, the expression

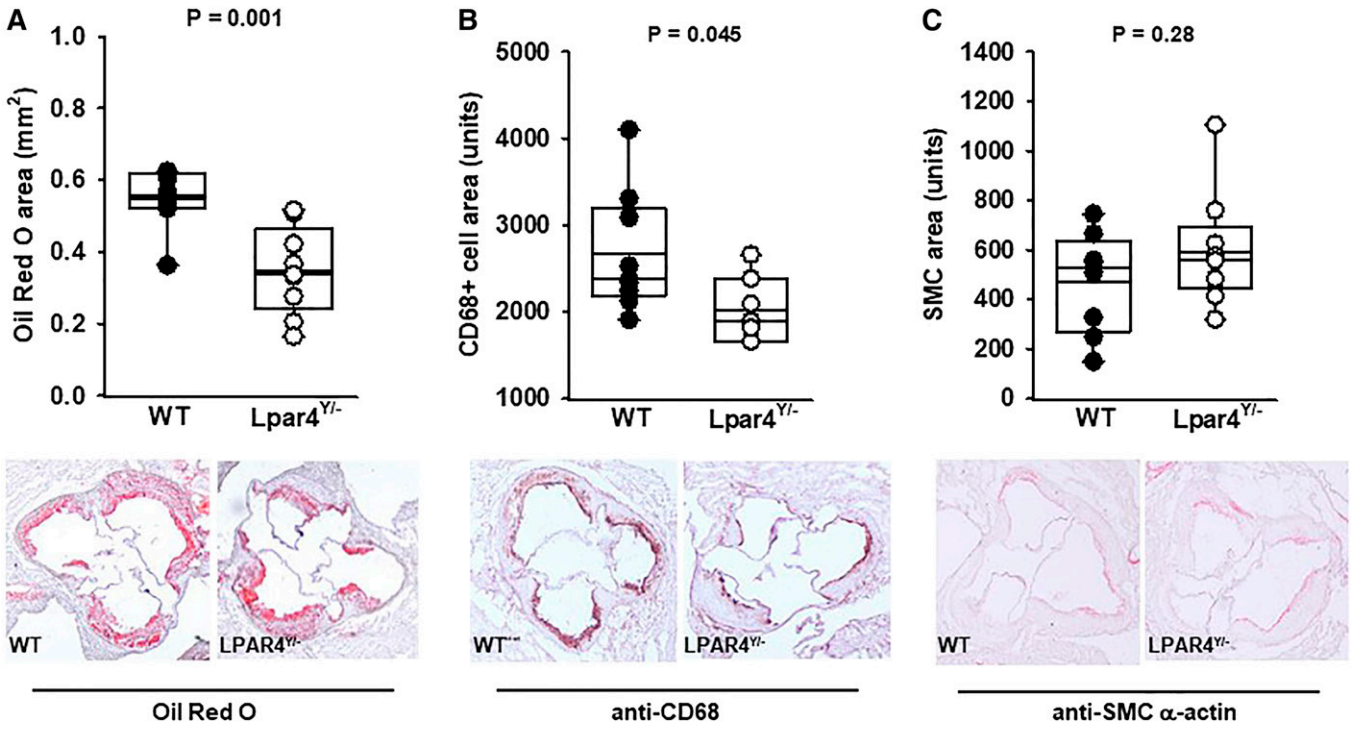

Fig. 2. LPAR4 deficiency in male mice reduces neutral lipid and CD68$^+$ cell content but not α-smooth muscle actin in aortic root atherosclerotic lesions. A: Quantification of lipid content (μm^2) from Oil Red O staining of aortas from individual WT (dark circles) or *Lpar4*$^{Y/-}$ (open circles) mice ($P = 0.001$) and representative Oil Red O staining of neutral lipid in aortic root sections (bottom). B: Quantification of CD68$^+$ staining from individual WT (dark circles) or *Lpar4*$^{Y/-}$ (open circles) mice ($P = 0.045$) and representative CD68$^+$ staining (bottom). C: Quantification of α-smooth muscle actin staining from individual WT (dark circles) or *Lpar4*$^{Y/-}$ (open circles) mice ($P = 0.27$) and representative α-smooth cell actin staining (bottom). In all cases, the area values for each mouse are the average of six measurements taken 80 μM apart.

of *Acta2*, which encodes α-smooth muscle actin, was lower at baseline in the knockout cells ($P = 0.001$ vs. WT). *Acta2* expression in SMCs declined further after ox-LDL exposure ($P = 0.001$ vs. vehicle control) and was lowest in *Lpar4*-deficient cells treated with ox-LDL. In contrast, the lack of LPAR4 did not appear to influence the α-smooth muscle actin area of expression by immunohistochemistry in sections of atherosclerosis (Fig. 2C). To determine whether there was a difference in lineage-committed SMCs in the atherosclerotic plaques, we used in situ hybridization and PLAs to visualize the H3K4dime marker of the MYH11 locus that is restricted to the SMC lineage (33). Quantification of the number of PLA$^+$ cells revealed a higher density of positive cells in atherosclerotic lesions at the aortic root of *Lpar4*$^{Y/-}$ mice (4.1 ± 1.3 PLA$^+$ cells per μm^2 area; $n = 8$) than WT mice (2.7 ± 1.1 PLA$^+$ cells per μm^2 area; $n = 9$; $P = 0.033$) (Fig. 4B, C, supplemental Fig. 4).

DISCUSSION

We have provided evidence that LPA receptor signaling contributes to the development of experimental atherosclerosis. Specifically, the lack of LPAR4, a receptor previously demonstrated to regulate vascular development in mice, attenuated atherosclerosis in male mice. The reduction in atherosclerosis was accompanied by less accumulation of CD68$^+$ cells, indicating a change in the inflammatory composition of the plaque. BMDMs isolated from LPAR4-deficient mice displayed a paradoxical upregulation of gene expression for the M2 macrophage marker ARG1 and the transcriptional regulator KLF4 when exposed to LPA. Immunohistochemical analysis confirmed heightened M2 markers in atherosclerotic lesions of LPAR4-deficient mice. Previous results from in vitro assays indicated that LPA increases neutral lipid accumulation in macrophages and prevents their reverse migration across an endothelial layer (17). It is possible that LPAR4 has a role in these events during the course of atherosclerosis as well as effects on inflammatory profiles.

Alternative M2 macrophages are induced in response to Th2-type cytokines IL-4 and IL-13 and secrete anti-inflammatory factors. In general, M2 macrophages tend to resolve plaque inflammation and promote tissue repair, in part by taking up and oxidizing fatty acids and secreting high levels of collagen. The transcription factor KLF4 promotes M2 and inhibits M1 macrophage polarization, and its absence accelerates atherosclerosis (45). LPA is known to regulate KLF4 (46) to affect cellular phenotypes. In cultured BMDMs, LPA4 appears to suppress LPA-mediated increases in KLF4 expression and, in the absence of the receptor, higher KLF4 expression could promote the M2 phenotype. Additional pathways that may be involved include CD14, which has been reported to be a key mediator of both LPA and lipopolysaccharide- induced foam cell formation in vitro (36). In addition, LPA promotes ox-LDL uptake

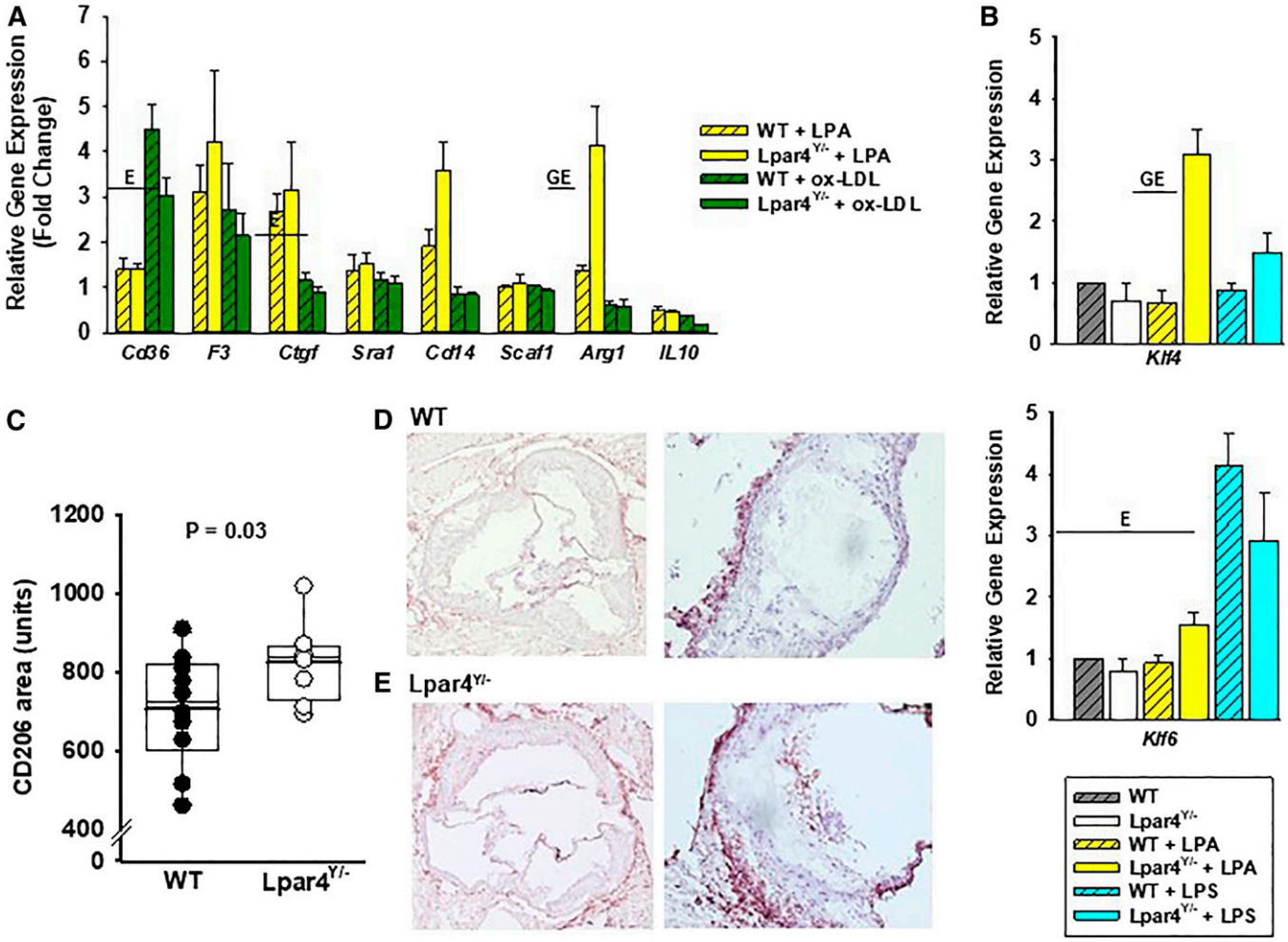

Fig. 3. LPAR4 deficiency influences oxidized LDL-elicited gene expression in BMDMs. A: Gene expression analysis in cells isolated from WT (open bars) or *Lpar4*$^{Y/-}$ (hatched bars) mice. Cells were harvested from four mice, cultured for 7 days, and then exposed to 18:1 LPA (5 μM; yellow bars), ox-LDL (50 μg/ml; green bars), or vehicle control for 3 h. Results are presented relative to the expression with vehicle exposure and are summarized from three separate experiments analyzed by two-way ANOVA with the Mann-Whitney test. E = significant differences in gene expression between environmental exposures ($P < 0.05$). GE = significant differences in gene expression based on genotype and environmental exposure ($P < 0.05$). B: *Klf4* and *Klf6* gene expression analysis in BMDMs isolated from WT (gray hatched bars; $n = 4$) or *Lpar4*$^{Y/-}$ (open bars; $n = 4$) exposed to vehicle control, 18:1 LPA (2 μM; yellow bars), or LPS (100 ng/ml; blue bars) for 3 h. Results are presented relative to expression with vehicle exposure and are summarized from three separate experiments analyzed by two-way ANOVA with the Mann-Whitney test. GE = significant differences in gene expression based on genotype and environmental exposure ($P < 0.05$). C: CD206^{+} staining in aortic root sections from WT (dark circles; $n = 10$) or *Lpar4*$^{Y/-}$ (open circles; $n = 8$) mice. Individual values represent the average of six measurements taken 80 μM apart ($P = 0.03$). D: Representative images of sections of WT aortic root stained for CD205 at 4× (left) and 20× (right). E: Representative images of sections of *Lpar4*$^{Y/-}$ aortic root stained for CD205 at 4× (left) and 20× (right). LPS, lipopolysaccharide.

through SRA-dependent mechanisms in macrophages (47). LPA has been proposed as a key molecule in serum responsible for SMC dedifferentiation (40) and has been shown to regulate SMC contraction through LPAR1 (48).

Intriguingly, aortic SMCs isolated from mice lacking LPAR4 displayed lower gene expression for α-smooth muscle actin basally and after ox-LDL exposure. However, we could not detect differences in SMCs in atherosclerotic lesions from the LPAR4-deficient mice. It is possible that differences in developmental origins of the SMCs in the two models could account for our findings. SMCs in the aortic root arise from the secondary heart field from lateral plate mesoderm, whereas the SMCs isolated from descending thoracic and abdominal aorta are from somites. In other contexts, we have observed differences in LPA signaling in SMCs from these developmentally distinct regions.

The reduction in atherosclerosis was independent of an effect on plasma lipoprotein content. This finding is different from observations with the LPAR1/3 antagonist Ki16425 that lacks activity at LPAR4, which also reduced experimental atherosclerosis in *Ldlr*$^{-/-}$ mice (8). Ki16425 mildly reduced total cholesterol in *Ldlr*$^{-/-}$ mice with a trend toward lowering LDL (24). LAPR1/3 antagonism also changed the inflammatory composition of the lesions by reducing monocyte and neutrophil accumulation and increasing regulatory T-cells. Together with our findings, these results support a role for LPAR signaling in promoting inflammation during atherosclerosis.

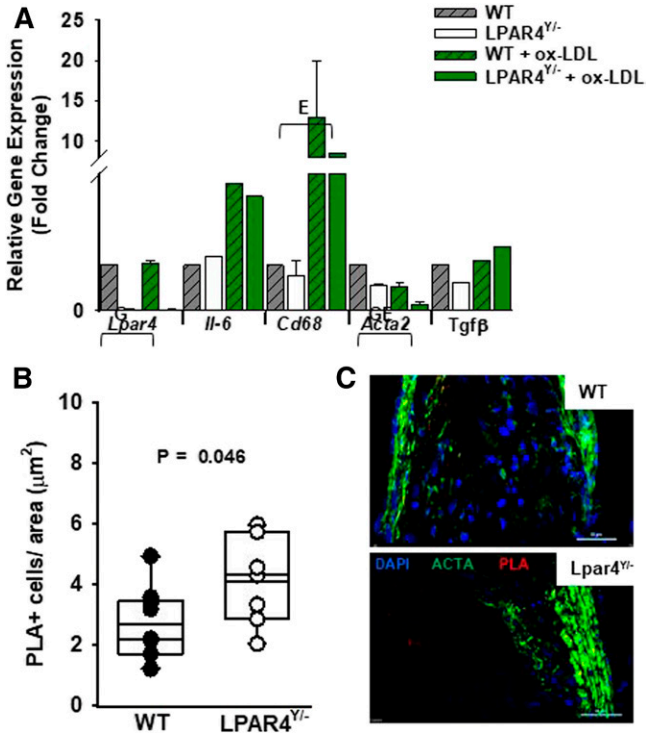

Fig. 4. LPAR4 deficiency influences ox-LDL-induced gene expression in aortic SMCs. A: Gene expression analysis from SMCs isolated from WT (gray hatched bars) or *Lpar4*$^{Y/-}$ (open bars) aortas. Cells were exposed to ox-LDL (50 μg/ml; green bars) or vehicle control for 3 h. Results are presented relative to expression in WT vehicle-treated cells and are summarized from three separate experiments analyzed by two-way ANOVA with the Mann-Whitney test. E = significant difference in gene expression between environmental exposures ($P < 0.05$). G = significant difference in gene expression between genotypes ($P < 0.05$). GE = significant difference in gene expression based on genotype and environmental exposure ($P < 0.05$). B: Quantification of MYH11 H3K4dime PLA^{+} cells from individual WT (dark circles) or *Lpar4*$^{Y/-}$ (open circles) mice. Individual values represent the average of six measurements taken 80 μM apart ($P = 0.045$). C: Representative immunostaining of aortic root sections from WT (top) and *Lpar4*$^{Y/-}$ (bottom) mice with DAPI (blue), ACTA2 (green), and MYH11 H3K4dime PLA signal (red). Scale bar = 50 μm.

In cellular models, considerable overlap between LPA receptors and their downstream signaling pathways has been reported (49). However, selective targeting of LPAR subtypes in mice and zebrafish yields distinct phenotypes, pointing to nonredundant roles for the receptors pathophysiologically (25, 26). Given the broad-ranging effects of LPA on cells and the observations with LPA receptor inhibitors, it seems that multiple LPA receptors contribute to experimental atherosclerosis. Receptor subtype expression in blood and vascular cells varies between humans and mice; for example, LPAR5 and LPAR6 are upregulated in human atheroma (50). Therefore, it is probably not possible to extrapolate the findings in mouse models directly to humans.

The downstream signaling pathways that mediate the effects of LPAR also demonstrate considerable overlap (49). Based on the similarities between the phenotypes in the LPAR4-deficient and Gα13-deficient mice (51), LPAR4 signaling regulating endothelial function has been suggested to go through this pathway (25). LPAR1 and LPAR6 have also been linked to Gα12/13 signaling (52). In mouse embryonic fibroblasts, LPAR4 appears to negatively regulate migration stimulated by an LPAR1-Gαi-PI3 kinase-dependent pathway, in that LPA4-deficient cells display enhanced migratory responses to LPA. The negative regulation of LPA signaling by LPAR4 in this model is similar to our observations of enhanced LPA responses in BMDMs lacking LPAR4. The downstream pathways mediating these effects are not known, although in addition to Gα12/13, Gαq and Gαs have also been proposed as mediating LPAR4 responses in other cells (53).

The role of LPA receptor signaling in experimental atherosclerosis certainly puts the pathway in a position to contribute to disease pathology in humans. Additionally, a role for LPA signaling in the development of atherosclerosis could explain the observations that a genetic variant, *PLPP3*, which encodes the LPA-inactivating enzyme LPP3, is strongly predictive of coronary artery disease and myocardial infarction in humans (54, 55). Furthermore, our results support the hypothesis that therapeutics targeting LPA pathways could be a novel anti-inflammatory approach to preventing complications of atherosclerotic disease.

REFERENCES

1. Choi, J. W., D. R. Herr, K. Noguchi, Y. C. Yung, C. W. Lee, T. Mutoh, M. E. Lin, S. T. Teo, K. E. Park, A. N. Mosley, et al. 2010. LPA receptors: subtypes and biological actions. *Annu. Rev. Pharmacol. Toxicol.* **50:** 157–186.
2. Moolenaar, W. H., and T. Hla. 2012. SnapShot: bioactive lysophospholipids. *Cell.* **148:** 378–378.e32.
3. Blaho, V. A., and T. Hla. 2011. Regulation of mammalian physiology, development, and disease by the sphingosine 1-phosphate and lysophosphatidic acid receptors. *Chem. Rev.* **111:** 6299–6320.
4. Tigyi, G. 2001. Physiological responses to lysophosphatidic acid and related glycero-phospholipids. *Prostaglandins Other Lipid Mediat.* **64:** 47–62.
5. Tigyi, G. 2008. Preface to the special issue: lysophospholipids in health and disease. *Biochim. Biophys. Acta.* **1781:** 423.
6. Panchatcharam, M., S. Miriyala, F. Yang, M. Rojas, C. End, C. Vallant, A. Dong, K. Lynch, J. Chun, A. J. Morris, et al. 2008. Lysophosphatidic acid receptors 1 and 2 play roles in regulation of vascular injury responses but not blood pressure. *Circ. Res.* **103:** 662–670.
7. Subramanian, P., E. Karshovska, P. Reinhard, R. T. Megens, Z. Zhou, S. Akhtar, U. Schumann, X. Li, M. van Zandvoort, C. Ludin, et al. 2010. Lysophosphatidic acid receptors LPA1 and LPA3 promote CXCL12-mediated smooth muscle progenitor cell recruitment in neointima formation. *Circ. Res.* **107:** 96–105.
8. Zhou, Z., P. Subramanian, G. Sevilmis, B. Globke, O. Soehnlein, E. Karshovska, R. Megens, K. Heyll, J. Chun, J. S. Saulnier-Blache, et al. 2011. Lipoprotein-derived lysophosphatidic acid promotes atherosclerosis by releasing CXCL1 from the endothelium. *Cell Metab.* **13:** 592–600.
9. Pamuklar, Z., J. S. Lee, H. Y. Cheng, M. Panchatcharam, S. Steinhubl, A. J. Morris, R. Charnigo, and S. S. Smyth. 2008. Individual heterogeneity in platelet response to lysophosphatidic acid: evidence for a novel inhibitory pathway. *Arterioscler. Thromb. Vasc. Biol.* **28:** 555–561.
10. Haserück, N., W. Erl, D. Pandey, G. Tigyi, P. Ohlmann, C. Ravanat, C. Gachet, and W. Siess. 2004. The plaque lipid lysophosphatidic acid stimulates platelet activation and platelet-monocyte aggregate formation in whole blood: involvement of P2Y1 and P2Y12 receptors. *Blood.* **103:** 2585–2592.
11. Morris, A. J., S. Selim, A. Salous, and S. S. Smyth. 2009. Blood relatives: dynamic regulation of bioactive lysophosphatidic acid

and sphingosine-1-phosphate metabolism in the circulation. *Trends Cardiovasc. Med.* **19:** 135–140.
12. Morris, A. J., M. Panchatcharam, H. Y. Cheng, L. Federico, Z. Fulkerson, S. Selim, S. Miriyala, D. Escalante-Alcalde, and S. S. Smyth. 2009. Regulation of blood and vascular cell function by bioactive lysophospholipids. *J. Thromb. Haemost.* **7 (Suppl. 1):** 38–43.
13. Schulze, C., C. Smales, L. L. Rubin, and J. M. Staddon. 1997. Lysophosphatidic acid increases tight junction permeability in cultured brain endothelial cells. *J. Neurochem.* **68:** 991–1000.
14. Tager, A. M., P. LaCamera, B. S. Shea, G. S. Campanella, M. Selman, Z. Zhao, V. Polosukhin, J. Wain, B. A. Karimi-Shah, N. D. Kim, et al. 2008. The lysophosphatidic acid receptor LPA1 links pulmonary fibrosis to lung injury by mediating fibroblast recruitment and vascular leak. *Nat. Med.* **14:** 45–54.
15. Olorundare, O. E., O. Peyruchaud, R. M. Albrecht, and D. F. Mosher. 2001. Assembly of a fibronectin matrix by adherent platelets stimulated by lysophosphatidic acid and other agonists. *Blood.* **98:** 117–124.
16. Smyth, S. S., H. Y. Cheng, S. Miriyala, M. Panchatcharam, and A. J. Morris. 2008. Roles of lysophosphatidic acid in cardiovascular physiology and disease. *Biochim. Biophys. Acta.* **1781:** 563–570.
17. Llodrá, J., V. Angeli, J. Liu, E. Trogan, E. A. Fisher, and G. J. Randolph. 2004. Emigration of monocyte-derived cells from atherosclerotic lesions characterizes regressive, but not progressive, plaques. *Proc. Natl. Acad. Sci. USA.* **101:** 11779–11784.
18. Siess, W., K. J. Zangl, M. Essler, M. Bauer, R. Brandl, C. Corrinth, R. Bittman, G. Tigyi, and M. Aepfelbacher. 1999. Lysophosphatidic acid mediates the rapid activation of platelets and endothelial cells by mildly oxidized low density lipoprotein and accumulates in human atherosclerotic lesions. *Proc. Natl. Acad. Sci. USA.* **96:** 6931–6936.
19. Siess, W. 2002. Athero- and thrombogenic actions of lysophosphatidic acid and sphingosine-1-phosphate. *Biochim. Biophys. Acta.* **1582:** 204–215.
20. Bot, M., I. Bot, R. Lopez-Vales, C. H. van de Lest, J. S. Saulnier-Blache, J. B. Helms, S. David, T. J. van Berkel, and E. A. Biessen. 2010. Atherosclerotic lesion progression changes lysophosphatidic acid homeostasis to favor its accumulation. *Am. J. Pathol.* **176:** 3073–3084.
21. Tokumura, A., Y. Kanaya, M. Kitahara, M. Miyake, Y. Yoshioka, and K. Fukuzawa. 2002. Increased formation of lysophosphatidic acids by lysophospholipase D in serum of hypercholesterolemic rabbits. *J. Lipid Res.* **43:** 307–315.
22. Dohi, T., K. Miyauchi, R. Ohkawa, K. Nakamura, M. Kurano, T. Kishimoto, N. Yanagisawa, M. Ogita, T. Miyazaki, A. Nishino, et al. 2013. Increased lysophosphatidic acid levels in culprit coronary arteries of patients with acute coronary syndrome. *Atherosclerosis.* **229:** 192–197.
23. Navab, M., G. Hough, G. M. Buga, F. Su, A. C. Wagner, D. Meriwether, A. Chattopadhyay, F. Gao, V. Grijalva, J. S. Danciger, et al. 2013. Transgenic 6F tomatoes act on the small intestine to prevent systemic inflammation and dyslipidemia caused by Western diet and intestinally derived lysophosphatidic acid. *J. Lipid Res.* **54:** 3403–3418.
24. Kritikou, E., G. H. van Puijvelde, T. van der Heijden, P. J. van Santbrink, M. Swart, F. H. Schaftenaar, M. J. Kroner, J. Kuiper, and I. Bot. 2016. Inhibition of lysophosphatidic acid receptors 1 and 3 attenuates atherosclerosis development in LDL-receptor deficient mice. *Sci. Rep.* **6:** 37585.
25. Sumida, H., K. Noguchi, Y. Kihara, M. Abe, K. Yanagida, F. Hamano, S. Sato, K. Tamaki, Y. Morishita, M. R. Kano, et al. 2010. LPA4 regulates blood and lymphatic vessel formation during mouse embryogenesis. *Blood.* **116:** 5060–5070.
26. Yukiura, H., K. Hama, K. Nakanaga, M. Tanaka, Y. Asaoka, S. Okudaira, N. Arima, A. Inoue, T. Hashimoto, H. Arai, et al. 2011. Autotaxin regulates vascular development via multiple lysophosphatidic acid (LPA) receptors in zebrafish. *J. Biol. Chem.* **286:** 43972–43983.
27. Takara, K., D. Eino, K. Ando, D. Yasuda, H. Naito, Y. Tsukada, T. Iba, T. Wakabayashi, F. Muramatsu, H. Kidoya, et al. 2017. Lysophosphatidic acid receptor 4 activation augments drug delivery in tumors by tightening endothelial cell-cell contact. *Cell Reports.* **20:** 2072–2086.
28. Eino, D., Y. Tsukada, H. Naito, Y. Kanemura, T. Iba, T. Wakabayashi, F. Muramatsu, H. Kidoya, H. Arita, N. Kagawa, et al. 2018. LPA4-mediated vascular network formation increases the efficacy of anti-PD-1 therapy against brain tumors. *Cancer Res.* **78:** 6607–6620.
29. Hata, E., N. Sasaki, A. Takeda, K. Tohya, E. Umemoto, N. Akahoshi, S. Ishii, K. Bando, T. Abe, K. Kano, et al. 2016. Lysophosphatidic acid receptors LPA4 and LPA6 differentially promote lymphocyte transmigration across high endothelial venules in lymph nodes. *Int. Immunol.* **28:** 283–292.
30. Igarashi, H., N. Akahoshi, T. Ohto-Nakanishi, D. Yasuda, and S. Ishii. 2015. The lysophosphatidic acid receptor LPA4 regulates hematopoiesis-supporting activity of bone marrow stromal cells. *Sci. Rep.* **5:** 11410.
31. Lee, Z., C. T. Cheng, H. Zhang, M. A. Subler, J. Wu, A. Mukherjee, J. J. Windle, C. K. Chen, and X. Fang. 2008. Role of LPA4/p2y9/GPR23 in negative regulation of cell motility. *Mol. Biol. Cell.* **19:** 5435–5445.
32. Daugherty, A., and S. C. Whitman. 2003. Quantification of atherosclerosis in mice. *Methods Mol. Biol.* **209:** 293–309.
33. Gomez, D., L. S. Shankman, A. T. Nguyen, and G. K. Owens. 2013. Detection of histone modifications at specific gene loci in single cells in histological sections. *Nat. Methods.* **10:** 171–177.
34. Zheng, H., Y. Fu, Y. Huang, X. Zheng, W. Yu, and W. Wang. 2017. mTOR signaling promotes foam cell formation and inhibits foam cell egress through suppressing the SIRT1 signaling pathway. *Mol. Med. Rep.* **16:** 3315–3323.
35. Chen, L., J. Zhang, X. Deng, Y. Liu, X. Yang, Q. Wu, and C. Yu. 2017. Lysophosphatidic acid directly induces macrophage-derived foam cell formation by blocking the expression of SRBI. *Biochem. Biophys. Res. Commun.* **491:** 587–594.
36. An, D., F. Hao, F. Zhang, W. Kong, J. Chun, X. Xu, and M. Z. Cui. 2017. CD14 is a key mediator of both lysophosphatidic acid and lipopolysaccharide induction of foam cell formation. *J. Biol. Chem.* **292:** 14391–14400.
37. Duong, C. Q., S. M. Bared, A. Abu-Khader, C. Buechler, A. Schmitz, and G. Schmitz. 2004. Expression of the lysophospholipid receptor family and investigation of lysophospholipid-mediated responses in human macrophages. *Biochim. Biophys. Acta.* **1682:** 112–119.
38. Zhou, Z., J. Niu, and Z. Zhang. 2010. The role of lysophosphatidic acid receptors in phenotypic modulation of vascular smooth muscle cells. *Mol. Biol. Rep.* **37:** 2675–2686.
39. Guo, H., N. Makarova, Y. Cheng, S. E, R. R. Ji, C. Zhang, P. Farrar, and G. Tigyi. 2008. The early- and late stages in phenotypic modulation of vascular smooth muscle cells: differential roles for lysophosphatidic acid. *Biochim. Biophys. Acta.* **1781:** 571–581.
40. Hayashi, K., M. Takahashi, W. Nishida, K. Yoshida, Y. Ohkawa, A. Kitabatake, J. Aoki, H. Arai, and K. Sobue. 2001. Phenotypic modulation of vascular smooth muscle cells induced by unsaturated lysophosphatidic acids. *Circ. Res.* **89:** 251–258.
41. Riquelme-Guzmán, C., O. Contreras, and E. Brandan. 2018. Expression of CTGF/CCN2 in response to LPA is stimulated by fibrotic extracellular matrix via the integrin/FAK axis. *Am. J. Physiol. Cell Physiol.* **314:** C415–C427.
42. Muehlich, S., N. Schneider, F. Hinkmann, C. D. Garlichs, and M. Goppelt-Struebe. 2004. Induction of connective tissue growth factor (CTGF) in human endothelial cells by lysophosphatidic acid, sphingosine-1-phosphate, and platelets. *Atherosclerosis.* **175:** 261–268.
43. Cui, M. Z., G. Zhao, A. L. Winokur, E. Laag, J. R. Bydash, M. S. Penn, G. M. Chisolm, and X. Xu. 2003. Lysophosphatidic acid induction of tissue factor expression in aortic smooth muscle cells. *Arterioscler. Thromb. Vasc. Biol.* **23:** 224–230.
44. Rahman, K., Y. Vengrenyuk, S. A. Ramsey, N. R. Vila, N. M. Girgis, J. Liu, V. Gusarova, J. Gromada, A. Weinstock, K. J. Moore, et al. 2017. Inflammatory Ly6Chi monocytes and their conversion to M2 macrophages drive atherosclerosis regression. *J. Clin. Invest.* **127:** 2904–2915.
45. Liao, X., N. Sharma, F. Kapadia, G. Zhou, Y. Lu, H. Hong, K. Paruchuri, G. H. Mahabeleshwar, E. Dalmas, N. Venteclef, et al. 2011. Kruppel-like factor 4 regulates macrophage polarization. *J. Clin. Invest.* **121:** 2736–2749.
46. Shin, S. H., Y. W. Kwon, S. C. Heo, G. O. Jeong, B. R. Kim, E. J. Seo, and J. H. Kim. 2014. Kruppel-like factor 4 mediates lysophosphatidic acid-stimulated migration and proliferation of PC3M prostate cancer cells. *Exp. Mol. Med.* **46:** e104.
47. Chang, C. L., H. Y. Hsu, H. Y. Lin, W. Chiang, and H. Lee. 2008. Lysophosphatidic acid-induced oxidized low-density lipoprotein uptake is class A scavenger receptor-dependent in macrophages. *Prostaglandins Other Lipid Mediat.* **87:** 20–25.
48. Dancs, P. T., E. Ruisanchez, A. Balogh, C. R. Panta, Z. Miklos, R. M. Nusing, J. Aoki, J. Chun, S. Offermanns, G. Tigyi, et al. 2017. LPA1 receptor-mediated thromboxane A2 release is responsible for

lysophosphatidic acid-induced vascular smooth muscle contraction. *FASEB J.* **31:** 1547–1555.
49. Yung, Y. C., N. C. Stoddard, and J. Chun. 2014. LPA receptor signaling: pharmacology, physiology, and pathophysiology. *J. Lipid Res.* **55:** 1192–1214.
50. Aldi, S., L. P. Matic, G. Hamm, D. van Keulen, D. Tempel, K. Holmstrom, A. Szwajda, B. S. Nielsen, V. Emilsson, R. Ait-Belkacem, et al. 2018. Integrated human evaluation of the lysophosphatidic acid pathway as a novel therapeutic target in atherosclerosis. *Mol. Ther. Methods Clin. Dev.* **10:** 17–28.
51. Ruppel, K. M., D. Willison, H. Kataoka, A. Wang, Y. W. Zheng, I. Cornelissen, L. Yin, S. M. Xu, and S. R. Coughlin. 2005. Essential role for Galpha13 in endothelial cells during embryonic development. *Proc. Natl. Acad. Sci. USA.* **102:** 8281–8286.
52. Yanagida, K., and S. Ishii. 2011. Non-Edg family LPA receptors: the cutting edge of LPA research. *J. Biochem.* **150:** 223–232.
53. Yanagida, K., S. Ishii, F. Hamano, K. Noguchi, and T. Shimizu. 2007. LPA4/p2y9/GPR23 mediates rho-dependent morphological changes in a rat neuronal cell line. *J. Biol. Chem.* **282:** 5814–5824.
54. Reschen, M. E., K. J. Gaulton, D. Lin, E. J. Soilleux, A. J. Morris, S. S. Smyth, and C. A. O'Callaghan. 2015. Lipid-induced epigenomic changes in human macrophages identify a coronary artery disease-associated variant that regulates PPAP2B expression through altered C/EBP-beta binding. *PLoS Genet.* **11:** e1005061.
55. Schunkert, H., I. R. Konig, S. Kathiresan, M. P. Reilly, T. L. Assimes, H. Holm, M. Preuss, A. F. Stewart, M. Barbalic, C. Gieger, et al. 2011. Large-scale association analysis identifies 13 new susceptibility loci for coronary artery disease. *Nat. Genet.* **43:** 333–338.